Biosensors and Bioelectronics 24 (2009) 1512–1517

Contents lists available at ScienceDirect

Biosensors and Bioelectronics

journal homepage: www.elsevier.com/locate/bios

Short communication

Nanotechnologic biosensor ellipsometry and biomarker pattern analysis in the evaluation of atherosclerotic risk profile

G. Siegel[a,e,*], M. Rodríguez[a], F. Sauer[a], C. Abletshauser[b], C. de Mey[c], K. Schötz[d], L. Ringstad[e], M. Malmsten[e], P. Schäfer[a]

[a] Charité – University Clinic Berlin, Institute of Physiology, D-14195 Berlin, Germany
[b] Novartis Pharma, D-90327 Nürnberg, Germany
[c] Applied Clinical Pharmacology Services (ACPS), D-55252 Mainz-Kastel, Germany
[d] Dr. Willmar Schwabe Pharmaceuticals, Preclinical Research, D-76227 Karlsruhe, Germany
[e] Department of Physical Chemistry, Institute of Pharmacy, S-75123 Uppsala, Sweden

ARTICLE INFO

Article history:
Received 6 May 2008
Received in revised form 8 July 2008
Accepted 4 August 2008
Available online 15 August 2008

Keywords:
Nanotechnologic biosensor ellipsometry
Biomarker pattern analysis
Atherosclerotic risk profile
Statins
ω-3 fatty acids
Ginkgo biloba

ABSTRACT

A proteoheparan sulfate coated, hydrophobic silica surface serves as lipoprotein receptor at which the Ca^{2+}-driven arteriosclerotic nanoplaque formation can be pursued by laser-based ellipsometry. Any lipoprotein from human blood can be very sensitively tested for its atherogenic properties. From the same blood sample, it is possible to determine the concentration and activity of a series of interacting biomarker molecules which, through a pattern analysis, allow to assess the state of health with respect to cardiovascular diseases. These two interlinked and complementary biosensors make a prospective cardio-cerebro-vascular risk stratification feasible, especially the sequelae of an underlying arteriosclerotic disease. Based on these diagnostic tools, an optimized therapy decision for the patient can be taken and the necessary preventive measures for the still healthy person.

1. Introduction

Within the general setting of the program of regenerative, diagnostic and therapeutic medicine, the salient focus and impact will be placed on the development of biofunctionalized materials for tissue engineering and regenerative medicine. These materials are mostly built up from degradable polymers or hybrid materials based on polymers, natural and/or tissue derived materials and inorganic materials. Biofunctionalization and development of nanostructured surfaces are tools to develop the necessary real-time exchange of information and matter between the biological system and the physical backbone material. One major area of research can be the development of biofunctionalized nanoparticles ("bionanosystems"), biomaterials for imaging and therapy – as new contrast agents or biomimetics for diagnostic purposes – and the use of nanotechnology fabrication tools in the synthesis process and the development of improved tissue-biomaterial interfaces. Another would be the construction of synthetic (bioactive) scaffolds for the regeneration of complex tissues, as cartilage, bone, blood vessels and nerves.

In westernized societies, atherosclerosis and its clinical sequelae heart disease and stroke are the underlying cause of about 50% of all deaths. Thus, the prevention or deceleration of atherogenesis is one of the most significant medical objectives since this is a matter of avoidance of myocardial and cerebral infarction. Epidemiological studies have revealed several important environmental and genetic risk factors associated with atherosclerosis (Paras et al., 2008; Libby, 2008). Although 'lifestyle risk factors' are taken into account in the guidelines, e.g., of the American Heart Association, unexpected deaths on grounds of heart or brain attack were again and again reported, even though the persons concerned were not rated as high-risk patients (Kavey et al., 2003; Sacco et al., 2006; Smith et al., 2006). Therefore, the guidelines were repeatedly actualized and extended, e.g., by Ca score determinations (Expert Panel/Writing Group, 2007; Kumanyika et al., 2008).

Through the complementary biosensor models presented here it is attempted to directly assess the cardio-cerebro-vascular risk. On the one hand, from the same patient's blood sample, the atherosclerotic nanoplaque formation can be measured by means of an ellipsometric approach and, on the other hand, additional information via determination and pattern analysis of a variety

* Corresponding author at: Charité – University Clinic Berlin, Institute of Physiology, D-14195 Berlin, Germany. Tel.: +49 30 84451685; fax: +49 30 84451684.
E-mail address: guenter.siegel@charite.de (G. Siegel).

0956-5663/$ – see front matter © 2008 Elsevier B.V. All rights reserved.
doi:10.1016/j.bios.2008.08.011

of biomarkers acquired on those risk factors which can lead to an increased nanoplaque formation. In the following, both biosensors as well as one measurement result each of a clinical trial are presented.

2. Subjects, materials and methods

2.1. Subjects and study design

This was part of a preventional, randomized, 12-week study comprising a 4-week dietary run-in phase followed by a study treatment period of 8 weeks, which was conducted in the Phase I–II study clinic of the UMHAPT "Zaritza Johanna" University Hospital, Sofia, Bulgaria. The project has been reviewed and approved by the local Ethics Committee and the Bulgarian Drug Agency. Eleven patients (2 male, 9 female) with early stage metabolic syndrome aged 26–48 years were recruited, provided that they fell within the additional inclusion criteria smoking (all patients) and blood lipoprotein(a) concentration >30 mg/dL (9 patients). After the first taking of a 45 mL blood sample, the standard therapy of the patients was 2×120 mg/d *Ginkgo biloba* special extract EGb 761 (Rökan® novo, Spitzner Arzneimittel, Ettlingen, Germany) over 2 months. No statins, no calcium antagonists and no nitrate compounds were given. No adverse events occurred and all the patients felt well during and after ginkgo intake. After 2-month medication, the second taking of a 45 mL blood sample was carried out. 1 mL of blood was required for the determinations in duplicate of all 13 biomarkers together, the remaining 44 mL for the preparation of the lipid fraction needed in the ellipsometry measurement.

2.2. Preparations and solutions

All experiments were carried out in a blood substitute solution. The normal blood substitute solution consisted of a Krebs solution simulating the extracellular ionic microenvironment of the proteoglycans and lipoproteins: Na^+ 151.16, K^+ 4.69, Ca^{2+} 2.52, Mg^{2+} 1.1, Cl^- 145.4, HCO_3^- 16.31 and $H_2PO_4^-$ 1.38 mmol/L (25 °C, pH 7.3). The Krebs solutions were gassed by 93% N_2/7% CO_2 to hinder VLDL/IDL/LDL oxidation (Siegel et al., 1999). The HS-PG preparation had a molecular weight of about 175 kDa as assessed by chromatography on Sephacryl S 400 columns calibrated with reference proteoglycans. Analytical data revealed an HS proportion of 82 g/100 g dry weight corresponding to four HS chains ($\sim 4 \times 36$ kDa) with an average sulfate content of 0.5 sulfate groups/disaccharide unit covalently linked to the protein core. The protein content (~35 kDa) was 18 g/100 g dry weight. Lipoproteins were isolated by sequential preparative ultracentrifugation essentially as described previously (Siegel et al., 2003).

2.3. Ellipsometry measurements in a bionanosystem

The adsorption of the lipoproteins and of HS-PG was monitored by *in situ* ellipsometry of a nanostructured surface, as detailed previously (Siegel et al., 1999, 2003). All measurements were carried out with an Optrel Multiskop (Optrel, Kleinmachnow, Germany) at 532 nm. Prior to adsorption, the ellipsometry measurements require a determination of the complex refractive index of the substrate (Malmsten, 1994). In the case of a layered substrate such as oxidized silicon a correct determination of the adsorbed layer thickness and mean refractive index requires a determination of the silicon bulk complex refractive index ($N_2 = n_2 - ik_2$) as well as of the thickness (d_1) and the refractive index (n_1) of the oxide layer. This is done by measuring the ellipsometric parameters Ψ and Δ in two different media, e.g., air and buffer. From the two sets of Ψ and Δ, n_2, k_2, d_1 and n_1 can be determined separately. The methyl layer is neglected for the methylated silica surfaces. Electrophoretic studies suggest such silanization only adds 0.5 nm or less to the double layer surface of shear (Burns et al., 1995). Similar results were obtained with ellipsometry. All measurements were performed by four-zone null ellipsometry in order to reduce effects of optical component imperfections. After optical analysis of the bare substrate surface, the proteoglycan solution was added to the cuvette, and the values of Ψ and Δ recorded. The adsorption was monitored in one zone, since the four-zone procedure is time-consuming and since corrections for component imperfections had already been performed. The maximal time-resolution between two measurements is 3–4 s. The adsorption temperature was 25 °C. Stirring was performed by a magnetic stirrer at about 300 rpm. A bulk concentration of 0.1 mg/mL proteoheparan sulfate (0.192 mmol/L in disaccharide units) and of VLDL/IDL/LDL at its native blood concentration in the patient were used throughout. Furthermore, the measurements were performed at different Ca^{2+} concentrations around those in the biological system. The normal blood substitute solution consisted of a Krebs solution.

From Ψ and Δ, the mean refractive index (n_f) and average thickness (δ_{el}) of the adsorbed layer were calculated numerically according to an optical four-layer model (Malmsten, 1994). It was previously shown that both, adsorbed amounts and adsorbed layer thicknesses, obtained with ellipsometry agree well with those obtained with other methods for proteins, polymers, and surfactants at model surfaces (Malmsten, 1994; Tiberg et al., 1994). The adsorbed amount (Γ) was obtained using values of the molar refractivity and the specific volume of 4.1 and 0.75, respectively. Throughout, the pH was kept around 7.38 by the bicarbonate/phosphate buffer, and by a continuous aeration of the cuvette solution (sample volume 5 mL) with a 93% N_2/7% CO_2 gas mixture (Aga, Sweden). The latter is included due to the necessity to keep the pH well regulated throughout these experiments in order to avoid both proteoglycan and lipoprotein degradation and calcium phosphate precipitation. As a physicochemical biosensor procedure, the ellipsometric technique is flawed by 5% at the most, so that reliable data could be expected for each patient. Further details can be found in earlier publications (Malmsten et al., 1993; Siegel et al., 1996).

2.4. MPO, oxLDL, 8-iso-$PGF_{2\alpha}$ and bilobalide determinations

The determination of myeloperoxidase (MPO) and oxidized low-density lipoprotein (oxLDL) were carried out by the MPO and the Oxidized LDL ELISAs (Mercodia, Uppsala, Sweden) using murine monoclonal anti-MPO antibodies and monoclonal antibodies 4E6 against oxidized apolipoprotein B molecules, respectively. 8-Isoprostane was determined after batch purification of the samples on 8-Isoprostane affinity sorbent (mouse anti-8-isoprostane covalently bound to Sepharose 4B, no. 416359, Cayman-Chemical, Ann Arbor, MI, USA) using a commercial EIA kit (Cayman no. 516351) according to the instructions of the manufacturer. The concentration of ginkgo-bilobalide in the VLDL/IDL/LDL particles after 2-month treatment of the patients was determined by a Varian 1200L GC-MS/MS Triple Quadrupole with GC CP 3800 (Varian, Darmstadt, Germany).

3. Results and discussion

3.1. Nanotechnologic biosensor ellipsometry

The bionanosystem presented can serve as a model for arteriosclerosis (Fig. 1). A hydrophobic methylated silica surface is coated by a monomolecular layer of isolated HS-PG depositing through its transmembrane hydrophobic core domain, thus rep-

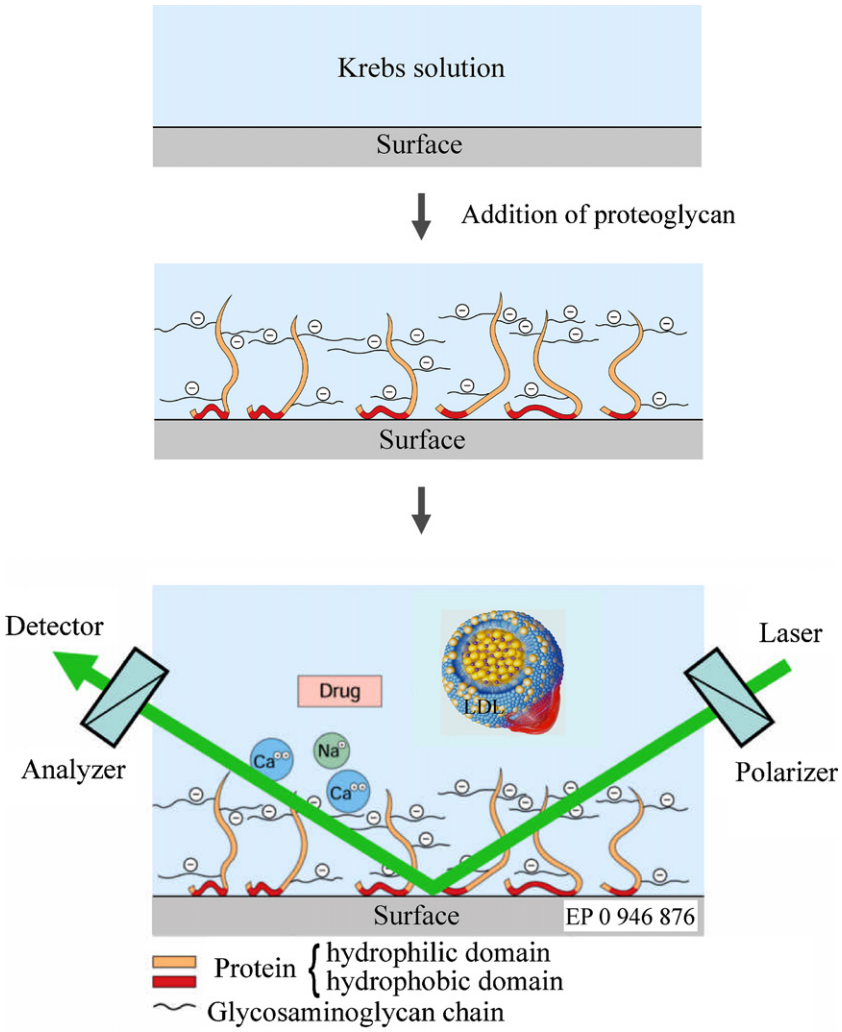

Fig. 1. Monomolecular coating of a methylated silica surface with proteoheparan sulfate molecules and their interaction both with Ca^{2+} and Na^{+} ions and lipoprotein particles in blood substitute solution (not to scale). Furthermore, the influence also of pharmaceuticals can be tested in this laser-based biosensor model (EP 0 946 876).

resenting a nano-structured surface mimicking endothelial cell membranes and extracellular matrices (patent EP 0 946 876) (Siegel and Malmsten, 2005). The glycosaminoglycan (GAG) side chains are stretched out into the blood substitute solution because of their negative fixed charges giving rise to electrostatic repulsion (Malmsten et al., 1994). Lipoprotein particles or cations may interact with the GAG chains, e.g., on occasion of their positive amino acid residues or simply their positive charges. The technical advantage of nanotechnologic biosensor ellipsometry for atherosclerotic risk stratification is highlighted by the fact that this method for the first time allows to measure the inclination to the very earliest stages of atherosclerotic plaque development of the entire atherogenic lipid fraction of a patient.

In a receptor-based biosensor application, this system was tested on its reliability to unveil possible pleiotropic effects of the CSE-inhibitor drugs fluvastatin, atorvastatin and simvastatin, the VLDL (triglyceride) lowering drug ω-3 fatty acids as well as the oxLDL and Lp(a) lowering phytochemical *G. biloba* (Siegel et al., 2003; Rodríguez et al., 2007; Ringstad et al., 2007). The objective of several clinical trials in cardiovascular high-risk patients (dyslipoproteinaemia and type 2 diabetes mellitus; aortocoronary bypass patients; metabolic syndrome; valvular defect operation) was to investigate the impact of a single dose of different statins, of a 2-month medication regimen of ω-3 fatty acids or of *G. biloba* (EGb 761) on nanoplaque formation and size. After a 4-week dietary run-in phase, the VLDL/IDL/LDL plasma fractions from the patients in these studies showed beginning nanoplaque formation already at a normal blood Ca^{2+} concentration (2.5 mmol/L), with a strong increase at higher Ca^{2+} concentrations. The drugs markedly slowed down this process to a variable extent. At 2.5 mmol/L Ca^{2+}, the mean relative reduction in nanoplaque formation and size was 10–60% and 20–80%, respectively, dependent upon the medicament given to the patients. In the present clinical trial with 11 metabolic syndrome patients we found in normal 2.52 mmol/L Ca^{2+} Krebs solution a reduction in nanoplaque formation (adsorbed amount) from 2.18 ± 0.11 to 1.87 ± 0.04 mg/m^2 ($p < 0.0077$, paired Student's *t*-test), i.e., by 14.3% after ginkgo treatment. Nanoplaque size (adsorbed layer thickness) decreased by 23.4%, from 33.89 ± 2.34 to 25.95 ± 1.86 nm ($p < 0.0004$, paired Student's *t*-test).

In Fig. 2, it is demonstrated how nanoplaque formation can be reduced although the total concentration of lipids and their subfractions remained constant after ginkgo medication. The results with the VLDL/IDL/LDL lipoprotein fraction in its natural blood concentration of one of the patients are illustrated. The lipid binding mechanism to HS-PG markedly changed after drug treatment, and

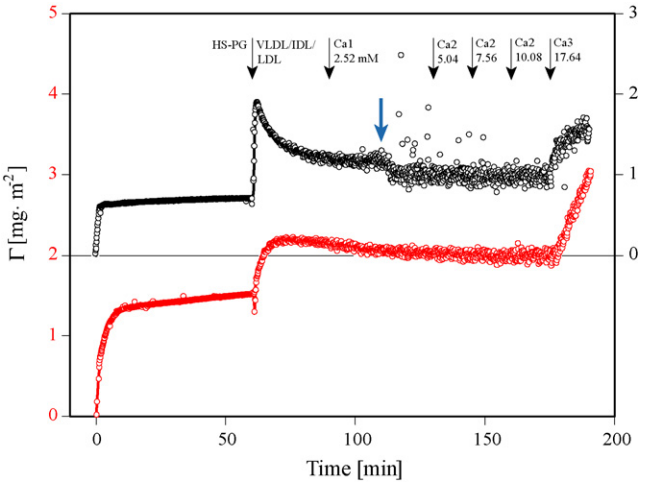

Fig. 2. Total adsorbed amount versus time. At time zero, HS-PG (0.1 mg/mL) was adsorbed on hydrophobic silica from a Ca^{2+}-free Krebs solution. The first arrow indicates the addition of the plasma VLDL/IDL/LDL fraction at its *in vivo* concentration from a metabolic syndrome patient either untreated (◯, black curve) or after 2 months treatment with daily 2 × 120 mg *G. biloba* extract (◯, red curve). Total Ca^{2+} concentrations in solution are indicated at the arrows. The thick blue arrow (↓) marks the visible beginning of HS-PG receptor destruction induced by oxVLDL/oxIDL/oxLDL. The thick, solid lines were computed by an iterative parameter fit of the nonlinear allosteric-cooperative, simple saturative or exponential kinetics to the experimental points using an algorithm for least-squares estimates. The pH was 7.35 (◯) and 7.27 (◯), respectively.

the general shape of the curve after Ca^{2+} additions was steeper downward after 2-month medication with ginkgo. However, the patient was selected for another reason. As can be easily seen, the stationary course of the baseline curve suddenly and for no obvious reason shows a downward deflection in the direction of desorption during the Ca1-addition (blue, thick arrow). Simultaneously, the scattering of the experimental points strongly increases. After ginkgo therapy, these changes could not be observed any longer.

From our measurements of the oxLDL/LDL ratio it resulted that this patient with 71.2 U/g had one of the highest oxLDL/LDL quotients of all the patients which exceeded their mean value by 19.0%. After ginkgo intake, oxLDL/LDL was reduced by 40.2%, thus lipid peroxidation limited. Ginkgo is a well-known and strong scavenger of oxygen free radicals (ROS) (Bridi et al., 2001; Chen et al., 2003; Ilieva et al., 2004; Zhou et al., 2006; Rodríguez et al., 2007). On the other hand, oxLDL itself is a cytotoxic radical that attacks proteins and lipids. Already in 2001 we found in ellipsometry investigations that oxLDL steadily reduced the adsorbed amount of the HS-PG/oxLDL complex and, furthermore, the scatter in the measurement rose significantly (Siegel et al., 2001). Possibly by its intervention as oxygen free radical, oxLDL seems to bind strongly to HS-PG and to alter its polyanionic GAG binding sites through breaking up the linkage β-D-glucuronic acid β(1 → 4) to *N*-acetyl-β-D-glucosamine as well as to change its protein backbone through peroxidation. The consequence is a dramatic increase in

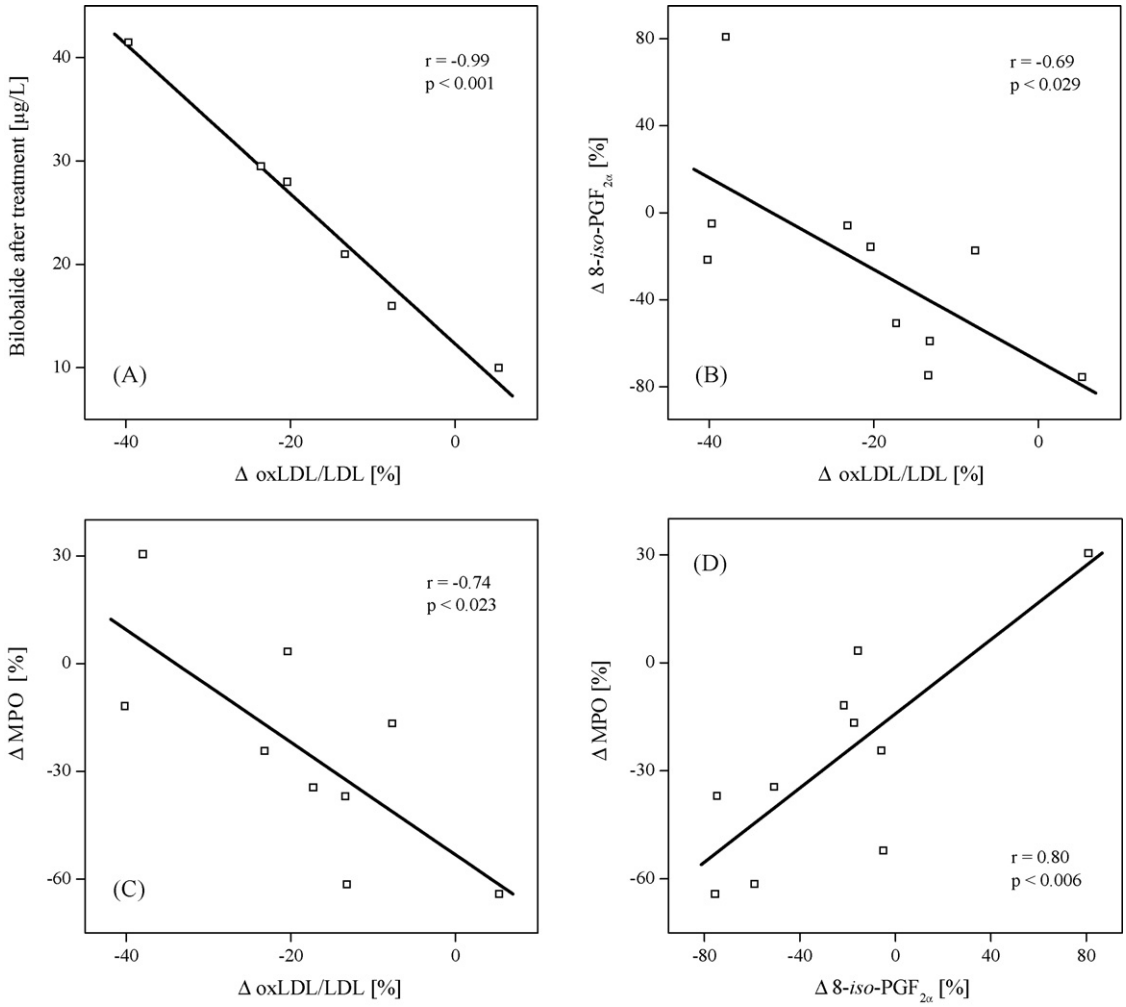

Fig. 3. Significant correlations between changes in bilobalide concentration in the VLDL/IDL/LDL particles (A), 8-*iso*-$PGF_{2\alpha}$ (B) and MPO (C) and changes in oxLDL/LDL ratio as well as between the changes in MPO and 8-*iso*-$PGF_{2\alpha}$ (D). For linear correlation analysis, Pearson's correlation coefficient *r* was calculated.

smaller, negatively charged particles (rise in scattering) that desorb from the silica surface. Altogether, this experiment impressively illustrates how sensitive this nanotechnologic biosensor assay functions, also as useful approach for further risk stratification in atherosclerosis.

3.2. Biomarker pattern analysis

Besides nanoplaque formation and size, a wide spectrum of parameters and biomarkers of oxidative stress, plaque stability and progression, inflammation, lipid composition including Lp(a) and second messengers was measured in the same blood samples of the patients that served for the ellipsometric measurements (Schäfer et al., 2007). As markers of oxidative stress, the isoprostane 8-*iso*-$PGF_{2\alpha}$, the ratio oxLDL/LDL and the activities of superoxide dismutase (SOD) and glutathione peroxidase (GPx) were determined. The inflammatory status was characterized by high-sensitivity C-reactive protein (hs-CRP), myeloperoxidase (MPO), tumor necrosis factor α (TNFα) and transforming growth factor β_1 (TGFβ_1). Furthermore, matrix metalloproteinase-9 (MMP-9) was measured as a relatively new marker to assess plaque stability. The biomarkers selected allowed a pattern analysis and are suited to provide a comprehensive risk profile assessment for the prevention of arteriosclerosis. Lipoprotein(a), genetically determined and fixed, 'independent' and potent atherothrombotic risk factor, is placed at a prominent site in the midst of the network of oxidative stress and inflammation parameters. Through biomarker array analysis based on individual correlation coefficients we could exemplarily show how an up-regulation in TNFα and TGFβ_1 in the lower physiologic regulatory range and a down-regulation in interleukin IL-6 and oxLDL/LDL ratio leads to the clinically highly relevant reduction in Lp(a) concentration of 26.3% under ginkgo treatment (Rodríguez et al., 2007). Furthermore, pattern analysis permits the prediction of biomarker and consequently cardiovascular disease (CVD) risk profile changes following an alteration of only one single parameter targeted by drug intervention.

Here, only one quartet from the biomarker pattern analysis shall be exemplarily demonstrated (Fig. 3). Fortunately, we were successful to identify the lipid-soluble leader substance bilobalide (terpene lactone) of the ginkgo extract EGb 761 in the VLDL/IDL/LDL lipoprotein particles of the patients after 2-month ginkgo treatment. Bilobalide is a powerful antioxidant and thus is locally concentrated exactly at the site in the body where it is imperative to inhibit lipid peroxidation in these metabolic syndrome patients. Therefore, we correlated the biomarkers and agents oxLDL/LDL, 8-*iso*-$PGF_{2\alpha}$ and MPO relevant for oxidative stress and obtained significant correlations in each case. One recognizes without difficulty that the reduction of the oxLDL/LDL quotient is so much the more extensive, the higher the bilobalide concentration in the lipid particles is (Fig. 3A). Another example shows that the MPO concentration decreases the more strongly, the more 8-*iso*-$PGF_{2\alpha}$ is reduced (Fig. 3D).

Oxidation, glycation, and desialylation are chemical processes that could modify LDL *in vivo*. The decrease in these cytotoxic particles may be a relevant mechanism which could support protection against CVD. Reduction in oxidative stress markers and mediators, such as 8-*iso*-$PGF_{2\alpha}$ and MPO, is beneficial since 8-*iso*-$PGF_{2\alpha}$, responsible for vasoconstriction and platelet aggregation, is especially accumulated in coronary arteries of coronary heart disease (CHD) patients (Mehrabi et al., 1999), and MPO, which is secreted during activation of neutrophils and monocytes, may serve as one mechanistic link among persistent inflammation, oxidative stress, and CVD (Stenvinkel et al., 2006). Serum levels of MPO, reducing NO release and inducing vasoconstriction, thus serving as a strong and independent predictor of endothelial dysfunction, powerfully predict an increased risk for subsequent cardiovascular events in patients with acute coronary syndrome.

4. Conclusion

The very earliest stage of atherogenesis on a molecular level, nanoplaque formation at the endothelial cell membrane and subendothelial extracellular matrices, can be measured with nanotechnologic biosensor ellipsometry. A nanoplaque is composed of the ternary aggregational complex proteoglycan – lipoprotein (VLDL, IDL, LDL, oxLDL, glyc-oxLDL) – calcium. Proteoglycans act as lipoprotein receptors, e.g., the membrane integral syndecan superfamily or the matrix proteins perlecan, decorin and biglycan (Abletshauser et al., 2002). The development of a biofunctionalized, nanostructured silica surface coated with a native proteoglycan isolated from the vascular wall, allows the binding of lipoproteins, taken from the patient's blood, in their natural concentration, as well as of Ca^{2+} ions. As shown exemplarily for oxLDL-LDL, the arteriosclerotic nanoplaque formation can be precisely measured by laser-based ellipsometric techniques. The concentration of selected biomarkers for oxidative stress, plaque stability and progression, and inflammation simultaneously determined in the blood of the patient, as well as of diagnostic parameters such as lipid composition including lipoprotein(a) and second messengers (cAMP, cGMP) makes it feasible, after flawless pattern analysis, to establish an arteriosclerotic risk profile of the patient and to tackle a further risk stratification with respect to future cardio-cerebro-vascular events.

References

Abletshauser, C., Klüßendorf, D., Schmidt, A., Winkler, K., März, W., Buddecke, E., Malmsten, M., Siegel, G., 2002. Acta Physiol. Scand. 176, 131–145.
Bridi, R., Crossetti, F.P., Steffen, V.M., Henriques, A.T., 2001. Phytother. Res. 15, 449–451.
Burns, N.L., van Alstine, J.M., Harris, J.M., 1995. Langmuir 11, 2768–2776.
Chen, J.-W., Chen, Y.-H., Lin, F.-Y., Chen, Y.-L., Lin, S.-J., 2003. Arterioscler. Thromb. Vasc. Biol. 23, 1559–1566.
Expert Panel/Writing Group, 2007. Circulation 115, 1481–1501.
Ilieva, I., Ohgami, K., Shiratori, K., Koyama, Y., Yoshida, K., Kase, S., Kitamei, H., Takemoto, Y., Yazawa, K., Ohno, S., 2004. Exp. Eye Res. 79, 181–187.
Kavey, R.-E.W., Daniels, S.R., Lauer, R.M., Atkins, D.L., Hayman, L.L., Taubert, K., 2003. Circulation 107, 1562–1566.
Kumanyika, S.K., Obarzanek, E., Stettler, N., Bell, R., Field, A.E., Fortmann, S.P., Franklin, B.A., Gillman, M.W., Lewis, C.E., Poston II, W.C., Stevens, J., Hong, Y., 2008. Circulation 118, 428–464.
Libby, P., 2008. J. Intern. Med. 263, 517–527.
Malmsten, M., 1994. J. Coll. Interface Sci. 166, 333–342.
Malmsten, M., Claesson, P., Siegel, G., 1994. Langmuir 10, 1274–1280.
Malmsten, M., Siegel, G., Buddecke, E., Schmidt, A., 1993. Coll. Surf. B: Biointerfaces 1, 43–50.
Mehrabi, M.R., Ekmekcioglu, C., Tatzber, F., Oguogho, A., Ullrich, R., Morgan, A., Tamaddon, F., Grimm, M., Glogar, H.D., Sinzinger, H., 1999. Cardiovasc. Res. 43, 492–499.
Paras, E., Mancini, G.B.J., Lear, S.A., 2008. Atherosclerosis 198, 228–236.
Ringstad, L., Winkler, K., Rodríguez, M., Malmsten, M., Siegel, G., 2007. Arterioscler. Thromb. Vasc. Biol. 27, e-102.
Rodríguez, M., Ringstad, L., Schäfer, P., Just, S., Hofer, H.W., Malmsten, M., Siegel, G., 2007. Atherosclerosis 192, 438–444.
Sacco, R.L., Adams, R., Albers, G., Alberts, M.J., Benavente, O., Furie, K., Goldstein, L.B., Gorelick, P., Halperin, J., Harbaugh, R., Johnston, S.C., Katzan, I., Kelly-Hayes, M., Kenton, E.J., Marks, M., Schwamm, L.H., Tomsick, T., 2006. Stroke 37, 577–617.
Schäfer, P., Rodríguez, M., Siegel, G., 2007. Atherosclerosis 195, 419–422.
Siegel, G., Abletshauser, C., Malmsten, M., Schmidt, A., Winkler, K., 2003. Cardiovasc. Res. 58, 696–705.
Siegel, G., Malmsten, M., 2005. Molecular model for athero/arteriosclerosis, patent EP 0 946 876.
Siegel, G., Malmsten, M., Klüßendorf, D., Leonhardt, W., 1999. Atherosclerosis 144, 59–67.
Siegel, G., Malmsten, M., Klüßendorf, D., Michel, F., 2001. Biosens. Bioelectron. 16, 895–904.

Siegel, G., Malmsten, M., Klüßendorf, D., Walter, A., Schnalke, F., Kauschmann, A., 1996. J. Auton. Nerv. Syst. 57, 207–213.
Smith Jr., S.C., Allen, J., Blair, S.N., Bonow, R.O., Brass, L.M., Fonarow, G.C., Grundy, S.M., Hiratzka, L., Jones, D., Krumholz, H.M., Mosca, L., Pasternak, R.C., Pearson, T., Pfeffer, M.A., Taubert, K.A., 2006. Circulation 113, 2363–2372.
Stenvinkel, P., Rodríguez-Ayala, E., Massy, Z.A., Qureshi, A.R., Barany, P., Fellström, B., Heimburger, O., Lindholm, B., Alvestrand, A., 2006. Clin. J. Am. Soc. Nephrol. 1, 281–287.
Tiberg, F., Jönsson, B., Tang, J., Lindman, B., 1994. Langmuir 10, 2294–2300.
Zhou, Y.-H., Yu, J.-P., Liu, Y.-F., Teng, X.-J., Ming, M., Lv, P., An, P., Liu, S.-Q., Yu, H.-G., 2006. Mediators Inflamm. 2006, 1–9.